Masses of doubly heavy tetraquarks $T_{QQ'}$ in a relativized quark model

Qi-Fang Lü[1,2,3,*] Dian-Yong Chen,[4,†] and Yu-Bing Dong[5,6,7,‡]

[1]*Department of Physics, Hunan Normal University, Changsha 410081, China*
[2]*Synergetic Innovation Center for Quantum Effects and Applications (SICQEA), Changsha 410081,China*
[3]*Key Laboratory of Low-Dimensional Quantum Structures and Quantum Control of Ministry of Education,*
Changsha 410081, China
[4]*School of Physics, Southeast University, Nanjing 210094, China*
[5]*Institute of High Energy Physics, Chinese Academy of Sciences, Beijing 100049, China*
[6]*Theoretical Physics Center for Science Facilities (TPCSF), CAS, Beijing 100049, China*
[7]*School of Physical Sciences, University of Chinese Academy of Sciences, Beijing 101408, China*

In the present work, the mass spectra of doubly heavy tetraquarks $T_{QQ'}$ are systematically investigated in a relativized quark model. The four-body systems including the Coulomb potential, confining potential, spin-spin interactions, and relativistic corrections are solved within the variational method. Our results suggest that the $IJ^P = 01^+$ $bb\bar{u}\bar{d}$ state is 54 MeV below the relevant $\bar{B}\bar{B}^*$ thresholds, which indicates that both strong and electromagnetic decays are forbidden, and thus this state can be a stable one. Its large hidden color component and small root mean square radius demonstrate that it is a compact tetraquark rather than a loosely bound molecule or pointlike diquark-antidiquark structure. Our predictions of the doubly heavy tetraquarks may provide valuable information for future experimental searches.

I. INTRODUCTION

In the past two decades, plenty of new resonances have been observed in the hadronic physics, and some of them can be hardly classified into the conventional hadron sectors, i.e., mesons and baryons [1]. These exotic structures have attracted extensive theoretical and experimental interests due to their enigmatic properties [2–12]. To describe their inner structures, new effective degrees of freedom are introduced to go beyond the traditional quark-antiquark and three-quark configurations. The experimental observations of charged quarkoniumlike states $Z_{c(b)}$ [13–17] and pentaquark states P_c [18,19] provide strong evidences for the existence of the exotic hadrons in QCD. Besides these hidden charm and bottom ones, it is also expected that the open flavor exotic states should exist. However, the experimental searches for these flavored exotic hadrons were beset with difficulties and obstacles, and the experiences of failures, such as $\Theta^+(1540)$ [20]

and $X(5568)$ [21,22], have cast a shadow over this research area.

The situation began to change in 2017, when a doubly heavy baryon Ξ_{cc}^{++} was observed by the LHCb Collaboration [23]. Although the Ξ_{cc}^{++} is regarded as a S-wave conventional baryon, it provides an excellent opportunity to examine the interactions between two heavy quarks and search for more doubly heavy quark systems. Indeed, based on the mass of Ξ_{cc}^{++}, the mass spectra of doubly heavy tetraquark states $T_{QQ'}$ were studied subsequently, which indicates that there should exist at least one stable flavored exotic tetraquark $bb\bar{u}\bar{d}$ [24,25].

Actually, the doubly heavy tetraquarks $T_{QQ'}$ have been discussed for a long time. Before the observation of Ξ_{cc}^{++}, there have been a number of theoretical works on the doubly heavy tetraquarks. Various approaches, involving quark models [24–42], QCD sum rules [43–46], and lattice QCD [47–50], were adopted to estimate their mass spectra. Due to the lack of experimental information on the doubly heavy systems, it is difficult to distinguish those numerous results. Also, several works have investigated their production mechanism, which should be helpful for experimental searches [51–55]. Lately, stimulated by the observation of Ξ_{cc}^{++}, the studies on doubly heavy systems were revived and have interested plenty of theorists and experimenters. In particular, the properties for the doubly heavy tetraquarks, such as their masses, decays, and production rates, have been extensively discussed in the

---
[*]lvqifang@hunnu.edu.cn
[†]chendy@seu.edu.cn
[‡]dongyb@ihep.ac.cn

past years [56–83]. Within different frameworks, these studies present distinctive results and conclusions. However, almost all the works agree that the isoscalar T_{bb} state should be stable against its strong and electromagnetic decays. The binding energy relative to the $\bar{B}\bar{B}^*$ threshold is predicted to be more than 100 MeV by most studies, which is deeply bound and leads to a compact configuration.

Within the framework of quark models, the previous studies were mainly based on the nonrelativistic quark potential models or simple quark models. Since the doubly heavy tetraquarks also include two light antiquarks, the relativistic corrections for the mass spectra may be significant. For instance, the masses of doubly heavy tetraquarks are calculated within a relativistic quark model under the diquark approximation [30]. However, the four-body calculations together with relativistic effects have not been done in the literature. Therefore, before making a final conclusion on the isoscalar T_{bb} state, it is essential to perform a calculation in a relativized quark model with few-body method for the doubly heavy tetraquark spectra.

In this paper, we investigate the mass spectra of doubly heavy tetraquarks $T_{QQ'}$ in the relativized quark model proposed by Godfrey, Capstick, and Isgur [84,85]. This model has been extensively adopted to study the properties of conventional hadrons and it may give a unified description of different flavor sectors. Also, under the diquark approximation, the authors have employed the relativized quark model to deal with the tetraquark states and achieved satisfactory results [86–92]. Thus, the relativized quark model is suitable for us to deal with the doubly heavy tetraquarks, where all the heavy-heavy, heavy-light, and light-light quark interactions are involved. For the first time, we extend the relativized quark model to investigate the double heavy tetraquark spectra by solving a four-body Schrödinger-type equation. With the present extension, the tetraquark, as well as the conventional hadrons can be described in a uniform frame.

This paper is organized as follows. The framework of relativized quark model and few-body method are introduced in Sec. II. The results and discussions of doubly heavy tetraquark spectra are given in Sec. III. A summary is presented in the last section.

II. MODEL

A. Hamiltonian

To calculate the mass spectra of doubly heavy tetraquarks $T_{QQ'} \equiv QQ'\bar{q}\bar{q}'$, the relativized Hamiltonian should be constructed. Similar to the procedures of the conventional mesons and baryons [84,85], the relativized Hamiltonian for a $QQ'\bar{q}\bar{q}'$ tetraquark state can be written as

$$H = H_0 + \sum_{i<j} V_{ij}^{\text{oge}} + \sum_{i<j} V_{ij}^{\text{conf}}, \tag{1}$$

where H_0 is a relativistic kinetic energy term

$$H_0 = \sum_{i=1}^{4} (p_i^2 + m_i^2)^{1/2}. \tag{2}$$

The V_{ij}^{oge} is the one gluon exchange pairwise potential, and V_{ij}^{conf} corresponds to the confining part. The kinematic energy of the center-of-mass system can be eliminated by the constraint $\sum_{i=1}^{4} \boldsymbol{p}_i = 0$.

In present work, we only concentrate on the S-wave ground states and do not include the spin-orbit and tensor interactions. Then, the potential V_{ij}^{oge} can be expressed as

$$V_{ij}^{\text{oge}} = \beta_{ij}^{1/2} \tilde{G}(r_{ij}) \beta_{ij}^{1/2} + \delta_{ij}^{1/2+\epsilon_c} \frac{2\boldsymbol{S}_i \cdot \boldsymbol{S}_j}{3m_i m_j} \nabla^2 \tilde{G}(r_{ij}) \delta_{ij}^{1/2+\epsilon_c}, \tag{3}$$

with

$$\beta_{ij} = 1 + \frac{p_{ij}^2}{(p_{ij}^2 + m_i^2)^{1/2}(p_{ij}^2 + m_j^2)^{1/2}}, \tag{4}$$

and

$$\delta_{ij} = \frac{m_i m_j}{(p_{ij}^2 + m_i^2)^{1/2}(p_{ij}^2 + m_j^2)^{1/2}}. \tag{5}$$

The p_{ij} is the magnitude of the momentum of either of the quarks in the center-of-mass frame of ij quark subsystem, and the ϵ_c is a free parameter reflecting the momentum dependence. The smeared Coulomb potential $\tilde{G}(r_{ij})$ is

$$\tilde{G}(r_{ij}) = \boldsymbol{F}_i \cdot \boldsymbol{F}_j \sum_{k=1}^{3} \frac{\alpha_k}{r_{ij}} \text{erf}(\tau_{kij} r_{ij}), \tag{6}$$

with

$$\frac{1}{\tau_{kij}^2} = \frac{1}{\gamma_k^2} + \frac{1}{\sigma_{ij}^2}, \tag{7}$$

and

$$\sigma_{ij}^2 = \sigma_0^2 \left[\frac{1}{2} + \frac{1}{2} \left(\frac{4m_i m_j}{(m_i + m_j)^2} \right)^4 \right] + s^2 \left(\frac{2m_i m_j}{m_i + m_j} \right)^2. \tag{8}$$

The $\boldsymbol{F}_i \cdot \boldsymbol{F}_j$ stands for the color matrix and reads

$$\boldsymbol{F}_i = \begin{cases} \frac{\lambda_i}{2} & \text{for quarks,} \\ -\frac{\lambda_i^*}{2} & \text{for antiquarks.} \end{cases} \tag{9}$$

Similarly, the confining interaction V_{ij}^{conf} can be expressed as

TABLE I. Relevant parameters of the relativized quark model [84].

m_u/m_d (MeV)	m_s (MeV)	m_c (MeV)	m_b (MeV)	α_1
220	419	1628	4977	0.25

α_2	α_3	γ_1 (GeV)	γ_2 (GeV)	γ_3 (GeV)
0.15	0.20	$1/2$	$\sqrt{10}/2$	$\sqrt{1000}/2$

b (GeV^2)	c (MeV)	σ_0 (GeV)	s	ϵ_c
0.18	-253	1.80	1.55	-0.168

$$V_{ij}^{\text{conf}} = -\frac{3}{4}\boldsymbol{F}_i \cdot \boldsymbol{F}_j$$
$$\times \left\{ br\left[\frac{e^{-\sigma_{ij}^2 r^2}}{\sqrt{\pi}\sigma_{ij}r} + \left(1 + \frac{1}{2\sigma_{ij}^2 r^2}\right)\text{erf}(\sigma_{ij}r)\right] + c\right\}. \tag{10}$$

All the parameters used here are taken from the original reference [84] and collected in Table I for convenience. These input parameters are obtained by fitting the low-lying meson spectra, and they allow us to describe the tetraquarks and conventional hadrons in a uniform frame. It should be mentioned that the actual accuracy of the relativized quark model depends on the quenched approximation and relativistic corrections. By considering these two effects, Ref. [84] claimed that the average accuracies are 25 MeV for light and heavy-light mesons and 10 MeV for heavy mesons, respectively. In fact, the constituent quark models only show the mass pattern rather than the

accurate values, and the model uncertainties can be hardly evaluated. Hence, people usually do not discuss the uncertainties within the framework of constituent quark model. In present work, only the ground states of doubly heavy tetraquarks are considered, and we expect that the uncertainties of predicted masses are limited in reasonable ranges. The details of the relativized procedure can be found in Refs. [84,85].

B. Matrix elements of color, flavor, and spin parts

The wave function of a $Q_1 Q_2' \bar{q}_3 \bar{q}_4'$ state can be divided into color, flavor, spin, and spatial parts. In the color space, one has two kinds of colorless states with well defined permutation properties,

$$|\bar{3}3\rangle = |(Q_1 Q_2')^{\bar{3}}(\bar{q}_3 \bar{q}_4')^3\rangle, \tag{11}$$

$$|6\bar{6}\rangle = |(Q_1 Q_2')^6(\bar{q}_3 \bar{q}_4')^{\bar{6}}\rangle, \tag{12}$$

where the $|\bar{3}3\rangle$ is antisymmetric under the exchange of both quarks and antiquarks, and the $|6\bar{6}\rangle$ is the symmetric one. One can evaluate the color matrix elements $\langle \boldsymbol{F}_i \cdot \boldsymbol{F}_j\rangle$ with the help of explicit color wave functions or the SU(3) Casimir operator. The results are collected in Table II.

For the flavor part, the combination between quarks $\bar{u}$ and $\bar{d}$ can be symmetric with $I = 1$ or antisymmetric with $I = 0$, while the combinations of $\bar{s}\,\bar{s}$, cc, and bb are always symmetric. For combinations $\bar{u}\,\bar{s}$ and $\bar{d}\,\bar{s}$, one can also construct the symmetric and antisymmetric flavor wave functions under the flavor SU(3) symmetry. The c and b are

TABLE II. Color matrix elements.

$\langle \hat{O}\rangle$	$\langle \boldsymbol{F}_1 \cdot \boldsymbol{F}_2\rangle$	$\langle \boldsymbol{F}_3 \cdot \boldsymbol{F}_4\rangle$	$\langle \boldsymbol{F}_1 \cdot \boldsymbol{F}_3\rangle$	$\langle \boldsymbol{F}_2 \cdot \boldsymbol{F}_4\rangle$	$\langle \boldsymbol{F}_1 \cdot \boldsymbol{F}_4\rangle$	$\langle \boldsymbol{F}_2 \cdot \boldsymbol{F}_3\rangle$
$\langle \bar{3}3|\hat{O}|\bar{3}3\rangle$	$-2/3$	$-2/3$	$-1/3$	$-1/3$	$-1/3$	$-1/3$
$\langle 6\bar{6}|\hat{O}|6\bar{6}\rangle$	$1/3$	$1/3$	$-5/6$	$-5/6$	$-5/6$	$-5/6$
$\langle \bar{3}3|\hat{O}|6\bar{6}\rangle$	0	0	$-1/\sqrt{2}$	$-1/\sqrt{2}$	$1/\sqrt{2}$	$1/\sqrt{2}$

TABLE III. Spin matrix elements.

$\langle \hat{O}\rangle$	$\langle \boldsymbol{S}_1 \cdot \boldsymbol{S}_2\rangle$	$\langle \boldsymbol{S}_3 \cdot \boldsymbol{S}_4\rangle$	$\langle \boldsymbol{S}_1 \cdot \boldsymbol{S}_3\rangle$	$\langle \boldsymbol{S}_2 \cdot \boldsymbol{S}_4\rangle$	$\langle \boldsymbol{S}_1 \cdot \boldsymbol{S}_4\rangle$	$\langle \boldsymbol{S}_2 \cdot \boldsymbol{S}_3\rangle$
$\langle \chi_0^{00}|\hat{O}|\chi_0^{00}\rangle$	$-3/4$	$-3/4$	0	0	0	0
$\langle \chi_0^{11}|\hat{O}|\chi_0^{11}\rangle$	$1/4$	$1/4$	$-1/2$	$-1/2$	$-1/2$	$-1/2$
$\langle \chi_0^{00}|\hat{O}|\chi_0^{11}\rangle$	0	0	$-\sqrt{3}/4$	$-\sqrt{3}/4$	$\sqrt{3}/4$	$\sqrt{3}/4$
$\langle \chi_1^{01}|\hat{O}|\chi_1^{01}\rangle$	$-3/4$	$1/4$	0	0	0	0
$\langle \chi_1^{10}|\hat{O}|\chi_1^{10}\rangle$	$1/4$	$-3/4$	0	0	0	0
$\langle \chi_1^{11}|\hat{O}|\chi_1^{11}\rangle$	$1/4$	$1/4$	$-1/4$	$-1/4$	$-1/4$	$-1/4$
$\langle \chi_1^{01}|\hat{O}|\chi_1^{10}\rangle$	0	0	$1/4$	$1/4$	$-1/4$	$-1/4$
$\langle \chi_1^{01}|\hat{O}|\chi_1^{11}\rangle$	0	0	$-\sqrt{2}/4$	$\sqrt{2}/4$	$-\sqrt{2}/4$	$\sqrt{2}/4$
$\langle \chi_1^{10}|\hat{O}|\chi_1^{11}\rangle$	0	0	$\sqrt{2}/4$	$-\sqrt{2}/4$	$-\sqrt{2}/4$	$\sqrt{2}/4$
$\langle \chi_2^{11}|\hat{O}|\chi_2^{11}\rangle$	$1/4$	$1/4$	$1/4$	$1/4$	$1/4$	$1/4$

treated as different particles and no symmetry constraint should be obeyed. For convenience, the notation $\bar{u}\bar{d}$ represents the combinations of $\bar{u}\bar{u}$, $\bar{d}\bar{d}$, $(\bar{u}\bar{d}+\bar{d}\bar{u})/\sqrt{2}$, and $(\bar{u}\bar{d}-\bar{d}\bar{u})/\sqrt{2}$, and notation $\bar{u}\bar{s}$ stands for the combinations $(\bar{u}\bar{s}+\bar{s}\bar{u})/\sqrt{2}$, $(\bar{u}\bar{s}-\bar{s}\bar{u})/\sqrt{2}$, $(\bar{d}\bar{s}+\bar{s}\bar{d})/\sqrt{2}$, and $(\bar{d}\bar{s}-\bar{s}\bar{d})/\sqrt{2}$ in the present work.

In the spin space, one can construct six spin states,

$$\chi_0^{00} = |(Q_1 Q_2')_0 (\bar{q}_3 \bar{q}_4')_0\rangle_0, \tag{13}$$

$$\chi_0^{11} = |(Q_1 Q_2')_1 (\bar{q}_3 \bar{q}_4')_1\rangle_0, \tag{14}$$

$$\chi_1^{01} = |(Q_1 Q_2')_0 (\bar{q}_3 \bar{q}_4')_1\rangle_1, \tag{15}$$

$$\chi_1^{10} = |(Q_1 Q_2')_1 (\bar{q}_3 \bar{q}_4')_0\rangle_1, \tag{16}$$

$$\chi_1^{11} = |(Q_1 Q_2')_1 (\bar{q}_3 \bar{q}_4')_1\rangle_1, \tag{17}$$

$$\chi_2^{11} = |(Q_1 Q_2')_1 (\bar{q}_3 \bar{q}_4')_1\rangle_2, \tag{18}$$

where $(Q_1 Q_2')_0$ and $(\bar{q}_3 \bar{q}_4')_0$ are antisymmetric for the two fermions under permutations, and the $(Q_1 Q_2')_1$ and $(\bar{q}_3 \bar{q}_4')_1$ are symmetric. For the notation $\chi_S^{S_{12} S_{34}}$, the S_{12}, S_{34}, and S are the spin of two heavy quarks, spin of two light antiquarks, and total spin, respectively. The relevant spin matrix elements can be evaluated with the standard angular momentum algebra, and the results are listed in Table III.

For a S-wave $T_{QQ'}$ state, the spatial part is always symmetric, and then the color-spin-flavor wave function should be antisymmetric for the identical quarks and antiquarks according to the Pauli exclusion principle. From the above discussions, we perform all possible configurations for the $QQ'\bar{q}\bar{q}'$ systems in Table IV. It should be noted that for a given system different configurations with same isospin-spin can mix with each other.

C. Matrix elements of spatial part

For a $Q_1 Q_2' \bar{q}_3 \bar{q}_4'$ state, the Jacobi coordinates are shown in Fig. 1. In these coordinates, one can define

$$\boldsymbol{r}_{12} = \boldsymbol{r}_1 - \boldsymbol{r}_2, \tag{19}$$

$$\boldsymbol{r}_{34} = \boldsymbol{r}_3 - \boldsymbol{r}_4, \tag{20}$$

$$\boldsymbol{r} = \frac{m_1 \boldsymbol{r}_1 + m_2 \boldsymbol{r}_2}{m_1 + m_2} - \frac{m_3 \boldsymbol{r}_3 + m_4 \boldsymbol{r}_4}{m_3 + m_4}, \tag{21}$$

and

$$\boldsymbol{R} = \frac{m_1 \boldsymbol{r}_1 + m_2 \boldsymbol{r}_2 + m_3 \boldsymbol{r}_3 + m_4 \boldsymbol{r}_4}{m_1 + m_2 + m_3 + m_4}. \tag{22}$$

TABLE IV. All possible configurations for the $QQ'\bar{q}\bar{q}'$ systems. The subscripts and superscripts are the spin quantum numbers and color types, respectively. The braces {}, brackets [] stand for the symmetric, antisymmetric flavor wave functions, respectively. The parentheses () are used for the subsystems without permutation symmetries.

System	IJ^P	Configuration		
$\{cc\}[\bar{u}\bar{d}]$	01^+	$|\{cc\}_1^{\bar{3}}[\bar{u}\bar{d}]_0^3\rangle_1$	$|\{cc\}_0^6[\bar{u}\bar{d}]_1^{\bar{6}}\rangle_1$	$\cdots$
$\{cc\}\{\bar{u}\bar{d}\}$	10^+	$|\{cc\}_1^{\bar{3}}\{\bar{u}\bar{d}\}_1^3\rangle_0$	$|\{cc\}_0^6\{\bar{u}\bar{d}\}_0^{\bar{6}}\rangle_0$	$\cdots$
	11^+	$|\{cc\}_1^{\bar{3}}\{\bar{u}\bar{d}\}_1^3\rangle_1$	$\cdots$	$\cdots$
	12^+	$|\{cc\}_1^{\bar{3}}\{\bar{u}\bar{d}\}_1^3\rangle_2$	$\cdots$	$\cdots$
$\{bb\}[\bar{u}\bar{d}]$	01^+	$|\{bb\}_1^{\bar{3}}[\bar{u}\bar{d}]_0^3\rangle_1$	$|\{bb\}_0^6[\bar{u}\bar{d}]_1^{\bar{6}}\rangle_1$	$\cdots$
$\{bb\}\{\bar{u}\bar{d}\}$	10^+	$|\{bb\}_1^{\bar{3}}\{\bar{u}\bar{d}\}_1^3\rangle_0$	$|\{bb\}_0^6\{\bar{u}\bar{d}\}_0^{\bar{6}}\rangle_0$	$\cdots$
	11^+	$|\{bb\}_1^{\bar{3}}\{\bar{u}\bar{d}\}_1^3\rangle_1$	$\cdots$	$\cdots$
	12^+	$|\{bb\}_1^{\bar{3}}\{\bar{u}\bar{d}\}_1^3\rangle_2$	$\cdots$	$\cdots$
$(cb)[\bar{u}\bar{d}]$	00^+	$|(cb)_0^{\bar{3}}[\bar{u}\bar{d}]_0^3\rangle_0$	$|(cb)_1^6[\bar{u}\bar{d}]_1^{\bar{6}}\rangle_0$	$\cdots$
	01^+	$|(cb)_1^{\bar{3}}[\bar{u}\bar{d}]_0^3\rangle_1$	$|(cb)_0^6[\bar{u}\bar{d}]_1^{\bar{6}}\rangle_1$	$|(cb)_1^6[\bar{u}\bar{d}]_1^{\bar{6}}\rangle_1$
	02^+	$|(cb)_1^6[\bar{u}\bar{d}]_1^{\bar{6}}\rangle_2$	$\cdots$	$\cdots$
$(cb)\{\bar{u}\bar{d}\}$	10^+	$|(cb)_0^{\bar{3}}\{\bar{u}\bar{d}\}_1^3\rangle_0$	$|(cb)_0^6\{\bar{u}\bar{d}\}_0^{\bar{6}}\rangle_0$	$\cdots$
	11^+	$|(cb)_0^{\bar{3}}\{\bar{u}\bar{d}\}_1^3\rangle_1$	$|(cb)_1^{\bar{3}}\{\bar{u}\bar{d}\}_1^3\rangle_1$	$|(cb)_1^6\{\bar{u}\bar{d}\}_0^{\bar{6}}\rangle_1$
	12^+	$|(cb)_1^{\bar{3}}\{\bar{u}\bar{d}\}_1^3\rangle_2$	$\cdots$	$\cdots$
$\{cc\}[\bar{u}\bar{s}]$	$\frac{1}{2}1^+$	$|\{cc\}_1^{\bar{3}}[\bar{u}\bar{s}]_0^3\rangle_1$	$|\{cc\}_0^6[\bar{u}\bar{s}]_1^{\bar{6}}\rangle_1$	$\cdots$
$\{cc\}\{\bar{u}\bar{s}\}$	$\frac{1}{2}0^+$	$|\{cc\}_1^{\bar{3}}\{\bar{u}\bar{s}\}_1^3\rangle_0$	$|\{cc\}_0^6\{\bar{u}\bar{s}\}_0^{\bar{6}}\rangle_0$	$\cdots$
	$\frac{1}{2}1^+$	$|\{cc\}_1^{\bar{3}}\{\bar{u}\bar{s}\}_1^3\rangle_1$	$\cdots$	$\cdots$
	$\frac{1}{2}2^+$	$|\{cc\}_1^{\bar{3}}\{\bar{u}\bar{s}\}_1^3\rangle_2$	$\cdots$	$\cdots$
$\{bb\}[\bar{u}\bar{s}]$	$\frac{1}{2}1^+$	$|\{bb\}_1^{\bar{3}}[\bar{u}\bar{s}]_0^3\rangle_1$	$|\{bb\}_0^6[\bar{u}\bar{s}]_1^{\bar{6}}\rangle_1$	$\cdots$
$\{bb\}\{\bar{u}\bar{s}\}$	$\frac{1}{2}0^+$	$|\{bb\}_1^{\bar{3}}\{\bar{u}\bar{s}\}_1^3\rangle_0$	$|\{bb\}_0^6\{\bar{u}\bar{s}\}_0^{\bar{6}}\rangle_0$	$\cdots$
	$\frac{1}{2}1^+$	$|\{bb\}_1^{\bar{3}}\{\bar{u}\bar{s}\}_1^3\rangle_1$	$\cdots$	$\cdots$
	$\frac{1}{2}2^+$	$|\{bb\}_1^{\bar{3}}\{\bar{u}\bar{s}\}_1^3\rangle_2$	$\cdots$	$\cdots$
$(cb)[\bar{u}\bar{s}]$	$\frac{1}{2}0^+$	$|(cb)_0^{\bar{3}}[\bar{u}\bar{s}]_0^3\rangle_0$	$|(cb)_1^6[\bar{u}\bar{s}]_1^{\bar{6}}\rangle_0$	$\cdots$
	$\frac{1}{2}1^+$	$|(cb)_1^{\bar{3}}[\bar{u}\bar{s}]_0^3\rangle_1$	$|(cb)_0^6[\bar{u}\bar{s}]_1^{\bar{6}}\rangle_1$	$|(cb)_1^6[\bar{u}\bar{s}]_1^{\bar{6}}\rangle_1$
	$\frac{1}{2}2^+$	$|(cb)_1^6[\bar{u}\bar{s}]_1^{\bar{6}}\rangle_2$	$\cdots$	$\cdots$
$(cb)\{\bar{u}\bar{s}\}$	$\frac{1}{2}0^+$	$|(cb)_0^{\bar{3}}\{\bar{u}\bar{s}\}_1^3\rangle_0$	$|(cb)_0^6\{\bar{u}\bar{s}\}_0^{\bar{6}}\rangle_0$	$\cdots$
	$\frac{1}{2}1^+$	$|(cb)_0^{\bar{3}}\{\bar{u}\bar{s}\}_1^3\rangle_1$	$|(cb)_1^{\bar{3}}\{\bar{u}\bar{s}\}_1^3\rangle_1$	$|(cb)_1^6\{\bar{u}\bar{s}\}_0^{\bar{6}}\rangle_1$
	$\frac{1}{2}2^+$	$|(cb)_1^{\bar{3}}\{\bar{u}\bar{s}\}_1^3\rangle_2$	$\cdots$	$\cdots$
$\{cc\}\{\bar{s}\bar{s}\}$	00^+	$|\{cc\}_1^{\bar{3}}\{\bar{s}\bar{s}\}_1^3\rangle_0$	$|\{cc\}_0^6\{\bar{s}\bar{s}\}_0^{\bar{6}}\rangle_0$	$\cdots$
	01^+	$|\{cc\}_1^{\bar{3}}\{\bar{s}\bar{s}\}_1^3\rangle_1$	$\cdots$	$\cdots$
	02^+	$|\{cc\}_1^{\bar{3}}\{\bar{s}\bar{s}\}_1^3\rangle_2$	$\cdots$	$\cdots$
$\{bb\}\{\bar{s}\bar{s}\}$	00^+	$|\{bb\}_1^{\bar{3}}\{\bar{s}\bar{s}\}_1^3\rangle_0$	$|\{bb\}_0^6\{\bar{s}\bar{s}\}_0^{\bar{6}}\rangle_0$	$\cdots$
	01^+	$|\{bb\}_1^{\bar{3}}\{\bar{s}\bar{s}\}_1^3\rangle_1$	$\cdots$	$\cdots$
	02^+	$|\{bb\}_1^{\bar{3}}\{\bar{s}\bar{s}\}_1^3\rangle_2$	$\cdots$	$\cdots$
$(cb)\{\bar{s}\bar{s}\}$	00^+	$|(cb)_1^{\bar{3}}\{\bar{s}\bar{s}\}_1^3\rangle_0$	$|(cb)_0^6\{\bar{s}\bar{s}\}_0^{\bar{6}}\rangle_0$	$\cdots$
	01^+	$|(cb)_0^{\bar{3}}\{\bar{s}\bar{s}\}_1^3\rangle_1$	$|(cb)_1^{\bar{3}}\{\bar{s}\bar{s}\}_1^3\rangle_1$	$|(cb)_1^6\{\bar{s}\bar{s}\}_0^{\bar{6}}\rangle_1$
	02^+	$|(cb)_1^{\bar{3}}\{\bar{s}\bar{s}\}_1^3\rangle_2$	$\cdots$	$\cdots$

Then, other relevant coordinates of this system can be expressed in terms of $\boldsymbol{r}_{12}$, $\boldsymbol{r}_{34}$, and $\boldsymbol{r}$ as follows:

$$\boldsymbol{r}_{13} = \boldsymbol{r}_1 - \boldsymbol{r}_3 = \frac{m_2}{m_1 + m_2}\boldsymbol{r}_{12} - \frac{m_4}{m_3 + m_4}\boldsymbol{r}_{34} + \boldsymbol{r}, \tag{23}$$
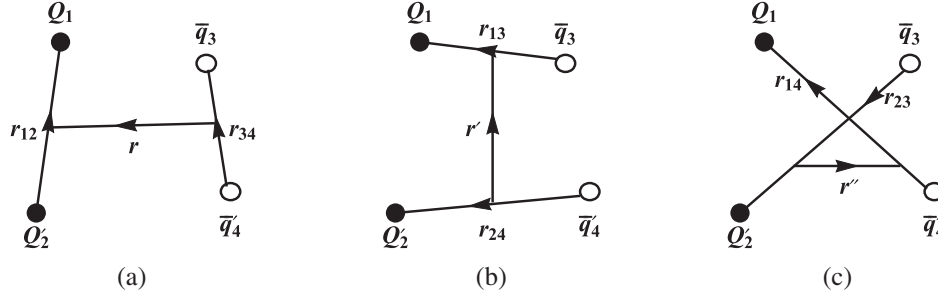
FIG. 1.   The $Q_1 Q_2' \bar{q}_3 \bar{q}_4'$ tetraquark state in Jacobi coordinates.

$$r_{24} = r_2 - r_4 = -\frac{m_1}{m_1 + m_2} r_{12} + \frac{m_3}{m_3 + m_4} r_{34} + r, \quad (24)$$

$$r_{14} = r_1 - r_4 = \frac{m_2}{m_1 + m_2} r_{12} + \frac{m_3}{m_3 + m_4} r_{34} + r, \quad (25)$$

$$r_{23} = r_2 - r_3 = -\frac{m_1}{m_1 + m_2} r_{12} - \frac{m_4}{m_3 + m_4} r_{34} + r, \quad (26)$$

$$
\begin{aligned}
r' &= \frac{m_1 r_1 + m_3 r_3}{m_1 + m_3} - \frac{m_2 r_2 + m_4 r_4}{m_2 + m_4} \\
&= \frac{m_1 m_2 (m_1 + m_2 + m_3 + m_4)}{(m_1 + m_2)(m_1 + m_3)(m_2 + m_4)} r_{12} \\
&\quad + \frac{m_3 m_4 (m_1 + m_2 + m_3 + m_4)}{(m_3 + m_4)(m_1 + m_3)(m_2 + m_4)} r_{34} \\
&\quad + \frac{m_1 m_4 - m_2 m_3}{(m_1 + m_3)(m_2 + m_4)} r,
\end{aligned}
\quad (27)
$$

$$
\begin{aligned}
r'' &= \frac{m_1 r_1 + m_4 r_4}{m_1 + m_4} - \frac{m_2 r_2 + m_3 r_3}{m_2 + m_3} \\
&= \frac{m_1 m_2 (m_1 + m_2 + m_3 + m_4)}{(m_1 + m_2)(m_1 + m_4)(m_2 + m_3)} r_{12} \\
&\quad - \frac{m_3 m_4 (m_1 + m_2 + m_3 + m_4)}{(m_3 + m_4)(m_1 + m_4)(m_2 + m_3)} r_{34} \\
&\quad + \frac{m_1 m_3 - m_2 m_4}{(m_1 + m_4)(m_2 + m_3)} r.
\end{aligned}
\quad (28)
$$

In our numerical calculation, the spatial wave function of a few-body system can be expanded in terms of a set of Gaussian basis functions, which forms an approximate complete set in a finite coordinate space [93]. For a S-wave $Q_1 Q_2' \bar{q}_3 \bar{q}_4'$ tetraquark, the expanded basis should satisfy the relation $l_{12} + l_{34} + l = 0$, where the l_{12}, l_{34}, and l are the relative angular momenta of the $Q_1 Q_2'$, $\bar{q}_3 \bar{q}_4'$, and $(Q_1 Q_2')(\bar{q}_3 \bar{q}_4')$, respectively. The contributions of higher orbital excitations to the ground states arise from the slight mixing via the spin-orbit or tensor interactions, which have been neglected in present calculations. Then, only the $l_{12} = l_{34} = l = 0$ case should be considered, and the spatial wave function for a certain tetraquark configuration can be expressed as

$$\Psi(r_{12}, r_{34}, r) = \sum_{n_Q, n_q, n} C_{n_Q n_q n} \psi_{n_Q}(r_{12}) \psi_{n_q}(r_{34}) \psi_n(r), \quad (29)$$

where $C_{n_Q n_q n}$ are the expansion coefficients. The $\psi_{n_Q}(r_{12}) \times \psi_{n_q}(r_{34}) \psi_n(r)$ stands for the position representation of the basis $|\alpha\rangle \equiv |n_Q n_q n\rangle$, where

$$\psi_n(r) = \frac{2^{7/4} \nu_n^{3/4}}{\pi^{1/4}} e^{-\nu_n r^2} Y_{00}(\hat{r}) = \left(\frac{2\nu_n}{\pi}\right)^{3/4} e^{-\nu_n r^2}, \quad (30)$$

$$\nu_n = \frac{1}{r_1^2 a^{2(n-1)}}, \quad (n = 1 - N_{\max}). \quad (31)$$

The three parameters r_1, a, and $N_{\max}$ are the Gaussian size parameters in geometric progression for numerical calculations, and the final results are stable and independent with these parameters within an approximate complete set in a sufficiently large space [93]. Besides the position representation $\psi_n(r)$, it is also convenient for the numerical calculations to present the momentum representation $\phi_n(p)$,

$$\phi_n(p) = \frac{2^{1/4}}{\pi^{1/4} \nu_n^{3/4}} e^{-p^2/(4\nu_n)} Y_{00}(\hat{p}) = \left(\frac{1}{2\pi\nu_n}\right)^{3/4} e^{-p^2/(4\nu_n)}. \quad (32)$$

Similarly, the formulas of $\psi_{n_Q}(r_{12})$, $\phi_{n_Q}(p_{12})$, $\psi_{n_q}(r_{34})$, and $\phi_{n_q}(p_{34})$ can be obtained by replacing the n, r, and p of the $\psi_n(r)$ and $\phi_n(p)$.

To calculate the spatial matrix elements, we encounter the momentum-dependent factors combined with the position-dependent potentials in the relativized Hamiltonian. This difficulty can be overcome by inserting complete sets of Gaussian functions between the two types of operators. Take the first term of V_{ij}^{oge}, for example, the matrix elements between two bases $|\alpha\rangle$ and $|\beta\rangle$ can be written as

$$
\langle \alpha | \beta_{ij}^{1/2} \tilde{G}(r_{ij}) \beta_{ij}^{1/2} | \beta \rangle = \sum_{\gamma, \delta, \rho, \lambda} \langle \alpha | \beta_{ij}^{1/2} | \gamma \rangle (N^{-1})_{\gamma\delta} \langle \delta | \tilde{G}(r_{ij}) | \rho \rangle \\
\times (N^{-1})_{\rho\lambda} \langle \lambda | \beta_{ij}^{1/2} | \beta \rangle. \quad (33)
$$

The N is the overlap matrix of the Gaussian functions with matrix elements $N_{ij} = \langle i|j \rangle$, which arises form the non-orthogonality of the bases. Together with the explicit forms of the basis in two representations, one can evaluate the expectations of momentum-dependent parts and position-dependent parts in the momentum representation and position representation, respectively.

D. Generalized eigenvalue problem

When all the matrix elements have been worked out, the mass spectra can be obtained by solving the generalized eigenvalue problem. For a given configuration without mixing, the homogeneous equation set can be expressed as

$$\sum_{j=1}^{N_{max}^3}(H_{ij} - EN_{ij})C_j = 0, \quad (i = 1 - N_{max}^3). \quad (34)$$

Where the H_{ij} are the matrix elements in the total color-flavor-spin-spatial bases, E stands for the eigenvalue, and C_j is the relevant eigenvector. The lowest eigenvalue represents the mass of this configuration, and the eigen-vector corresponds to the expansion coefficients $C_{n_\rho n_q n}$ in the spatial wave function.

From Table IV, a given system may include several different configurations with same IJ^P, which can mix with each other. In present calculation, we first solve the generalized eigenvalue problem to get the masses of pure configurations, and then calculate the off-diagonal effects between different configurations. The final mass spectra can be obtained by diagonalizing the mass matrix of these configurations.

III. RESULTS AND DISCUSSIONS

A. Numerical stability

Before discussing the properties of predicted tetraquarks, It is important to concentrate on the stabilities of the numerical procedures. In the nonrelativistic quark model, one can calculate the expectations of Hamiltonian in the trial wave functions, and always obtain the upper limit of the masses. When the number of bases increases, the numerical results decrease and approximate closely to the actual values. Empirically, stable results for S-wave states can be achieved within small numbers of bases.

In the relativized quark model, to calculate the matrix elements of Hamiltonian, complete sets of Gaussian functions should be inserted twice for the V_{ij}^{oge}, while the V_{ij}^{conf} and relativistic kinetic energy term can be evaluated straightforwardly. The number of bases should be large enough to guarantee approximate completeness, otherwise the matrix elements of V_{ij}^{oge} terms will be meaningless. For the meson spectra, a dozen bases are adequate, while about one hundred bases are needed for the baryon spectra [84,85]. One can expect that several hundred or one
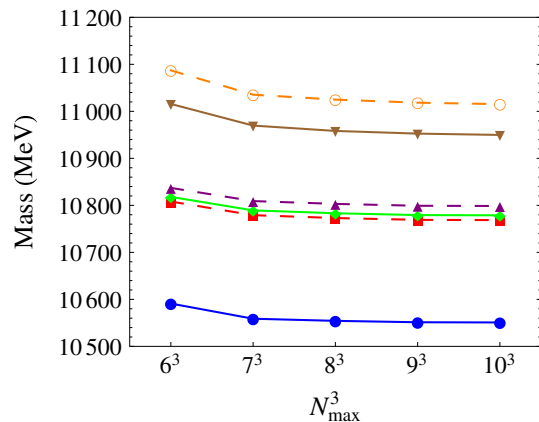
FIG. 2. Numerical stabilities for six pure configurations of $bb\bar{u}\bar{d}$ system. The blue points, red squares, green diamonds, purple triangles, brown inverted triangles, and orange circles stand for the $|\{bb\}_1^{\bar{3}}[\bar{u}\bar{d}]_0^3\rangle_1$, $|\{bb\}_1^{\bar{3}}\{\bar{u}\bar{d}\}_1^3\rangle_0$, $|\{bb\}_1^{\bar{3}}\{\bar{u}\bar{d}\}_1^3\rangle_1$, $|\{bb\}_1^{\bar{3}}\{\bar{u}\bar{d}\}_1^3\rangle_2$, $|\{bb\}_0^6[\bar{u}\bar{d}]_1^{\bar{6}}\rangle_1$, and $|\{bb\}_0^6\{\bar{u}\bar{d}\}_0^{\bar{6}}\rangle_0$ configurations.

thousand Gaussian functions are proper for calculating the tetraquark spectra.

Take the six pure configurations of $bb\bar{u}\bar{d}$ system for example, we investigate the dependence of results on the number of bases. The basis number varies from $N_{max}^3 = 6^3$ to 10^3, and the dependence is presented in Fig. 2. It is found that the eigenvalues are stable when the N_{max}^3 becomes larger. With $N_{max}^3 = 10^3$ bases, the numerical uncertainties are rather small, which are enough for the quark model calculations. Thus, we adopt 10^3 Gaussian bases to study the S-wave $T_{QQ'}$ spectra in present work.

B. Nonstrange systems

The predicted masses of $cc\bar{u}\bar{d}$, $bb\bar{u}\bar{d}$, and $cb\bar{u}\bar{d}$ systems are presented in Table V and Fig. 3. For the $cc\bar{u}\bar{d}$ system, the lowest state is the $IJ^P = 01^+$ one with 4041 MeV, which is a mixing state of the $|\{cc\}_1^{\bar{3}}[\bar{u}\bar{d}]_0^3\rangle_1$ and $|\{cc\}_0^6[\bar{u}\bar{d}]_1^{\bar{6}}\rangle_1$ configurations. This mixing is relatively small, and the $|\{cc\}_1^{\bar{3}}[\bar{u}\bar{d}]_0^3\rangle_1$ component is predominant. Due to the quantum conservation, the 0^+ and 2^+ states might decay into a pair of pseudoscalar mesons, while the allowed decay mode of a 1^+ state should be a vector meson plus a pseudoscalar one. From Fig. 3, it can be seen that the lowest $cc\bar{u}\bar{d}$ state is 165 MeV higher than the DD^* threshold, which can easily decay via falling apart mechanism.

For the $bb\bar{u}\bar{d}$ system, the mixing between different configurations is rather small and can be neglected. The predicted mass of the lowest state is 10550 MeV, which is almost a pure $|\{bb\}_1^{\bar{3}}[\bar{u}\bar{d}]_0^3\rangle_1$ state. From our calculation, its mass is lower than the $\bar{B}\bar{B}$ and $\bar{B}\bar{B}^*$ thresholds, which indicates that both strong and electromagnetic decays are

TABLE V.   Predicted mass spectra for the $cc\bar{u}\bar{d}$, $bb\bar{u}\bar{d}$, and $cb\bar{u}\bar{d}$ systems.

IJ^P	Configuration	$\langle H\rangle$ (MeV)	Mass (MeV)	Eigenvector
01^+	$\lvert\{cc\}_1^{\bar{3}}[\bar{u}\bar{d}]_0^3\rangle_1$ $\lvert\{cc\}_0^6[\bar{u}\bar{d}]_1^{\bar{6}}\rangle_1$	$\begin{pmatrix}4053 & -55\\ -55 & 4302\end{pmatrix}$	$\begin{bmatrix}4041\\ 4313\end{bmatrix}$	$\begin{bmatrix}(-0.979,-0.205)\\ (0.205,-0.979)\end{bmatrix}$
10^+	$\lvert\{cc\}_1^{\bar{3}}\{\bar{u}\bar{d}\}_1^3\rangle_0$ $\lvert\{cc\}_0^6\{\bar{u}\bar{d}\}_0^{\bar{6}}\rangle_0$	$\begin{pmatrix}4241 & -89\\ -89 & 4369\end{pmatrix}$	$\begin{bmatrix}4195\\ 4414\end{bmatrix}$	$\begin{bmatrix}(-0.890,-0.455)\\ (0.455,-0.890)\end{bmatrix}$
11^+	$\lvert\{cc\}_1^{\bar{3}}\{\bar{u}\bar{d}\}_1^3\rangle_1$	4268	4268	1
12^+	$\lvert\{cc\}_1^{\bar{3}}\{\bar{u}\bar{d}\}_1^3\rangle_2$	4318	4318	1
01^+	$\lvert\{bb\}_1^{\bar{3}}[\bar{u}\bar{d}]_0^3\rangle_1$ $\lvert\{bb\}_0^6[\bar{u}\bar{d}]_1^{\bar{6}}\rangle_1$	$\begin{pmatrix}10551 & 20\\ 20 & 10950\end{pmatrix}$	$\begin{bmatrix}10550\\ 10951\end{bmatrix}$	$\begin{bmatrix}(-0.999,0.050)\\ (-0.050,-0.999)\end{bmatrix}$
10^+	$\lvert\{bb\}_1^{\bar{3}}\{\bar{u}\bar{d}\}_1^3\rangle_0$ $\lvert\{bb\}_0^6\{\bar{u}\bar{d}\}_0^{\bar{6}}\rangle_0$	$\begin{pmatrix}10769 & 31\\ 31 & 11015\end{pmatrix}$	$\begin{bmatrix}10765\\ 11019\end{bmatrix}$	$\begin{bmatrix}(-0.993,0.122)\\ (-0.122,-0.993)\end{bmatrix}$
11^+	$\lvert\{bb\}_1^{\bar{3}}\{\bar{u}\bar{d}\}_1^3\rangle_1$	10779	10779	1
12^+	$\lvert\{bb\}_1^{\bar{3}}\{\bar{u}\bar{d}\}_1^3\rangle_2$	10799	10799	1
00^+	$\lvert(cb)_0^{\bar{3}}[\bar{u}\bar{d}]_0^3\rangle_0$ $\lvert(cb)_1^6[\bar{u}\bar{d}]_1^{\bar{6}}\rangle_0$	$\begin{pmatrix}7314 & -67\\ -67 & 7563\end{pmatrix}$	$\begin{bmatrix}7297\\ 7580\end{bmatrix}$	$\begin{bmatrix}(-0.970,-0.245)\\ (0.245,-0.970)\end{bmatrix}$
01^+	$\lvert(cb)_1^{\bar{3}}[\bar{u}\bar{d}]_0^3\rangle_1$ $\lvert(cb)_0^6[\bar{u}\bar{d}]_1^{\bar{6}}\rangle_1$ $\lvert(cb)_1^6[\bar{u}\bar{d}]_1^{\bar{6}}\rangle_1$	$\begin{pmatrix}7330 & -35 & 17\\ -35 & 7658 & 18\\ 17 & 18 & 7611\end{pmatrix}$	$\begin{bmatrix}7325\\ 7607\\ 7666\end{bmatrix}$	$\begin{bmatrix}(-0.992,-0.109,0.067)\\ (0.095,-0.274,0.957)\\ (-0.086,0.956,0.282)\end{bmatrix}$
02^+	$\lvert(cb)_1^6[\bar{u}\bar{d}]_1^{\bar{6}}\rangle_2$	7697	7697	1
10^+	$\lvert(cb)_1^{\bar{3}}\{\bar{u}\bar{d}\}_1^3\rangle_0$ $\lvert(cb)_0^6\{\bar{u}\bar{d}\}_0^{\bar{6}}\rangle_0$	$\begin{pmatrix}7535 & -56\\ -56 & 7724\end{pmatrix}$	$\begin{bmatrix}7519\\ 7740\end{bmatrix}$	$\begin{bmatrix}(-0.964,-0.265)\\ (0.265,-0.964)\end{bmatrix}$
11^+	$\lvert(cb)_0^6\{\bar{u}\bar{d}\}_1^3\rangle_1$ $\lvert(cb)_1^{\bar{3}}\{\bar{u}\bar{d}\}_1^3\rangle_1$ $\lvert(cb)_1^6\{\bar{u}\bar{d}\}_0^{\bar{6}}\rangle_1$	$\begin{pmatrix}7553 & 10 & 32\\ 10 & 7552 & -16\\ 32 & -16 & 7722\end{pmatrix}$	$\begin{bmatrix}7537\\ 7561\\ 7729\end{bmatrix}$	$\begin{bmatrix}(-0.740,0.648,0.183)\\ (-0.650,-0.758,0.054)\\ (-0.174,0.079,-0.982)\end{bmatrix}$
12^+	$\lvert(cb)_1^{\bar{3}}\{\bar{u}\bar{d}\}_1^3\rangle_2$	7586	7586	1

forbidden. Compared with $\bar{B}\bar{B}^*$ channel, the binding energy is 54 MeV and the decay width should be tiny enough. Although the binding energy is smaller than that of the nonrelativistic quark models [31,32,37–39,63,67, 71,73,78,79], we obtain the same conclusion about the stability of this state. The differences may arise from the relativized Hamiltonian, where the smearing potentials and relativistic corrections are included. This narrow structure can be searched via final states of weak decays, such as $\bar{B}D\pi^-$ and $\bar{B}Dl^-\nu_l$, in future LHC experiments [94,95].

For the $cb\bar{u}\bar{d}$ system, there are two lower states around 7.3 GeV. With small mixing, these two states mainly
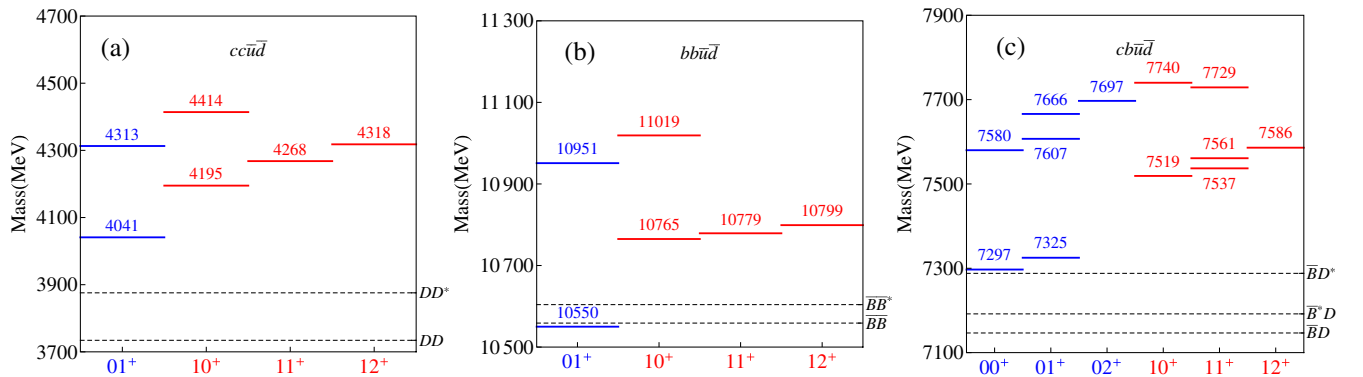
FIG. 3.   The predicted masses of $cc\bar{u}\bar{d}$, $bb\bar{u}\bar{d}$, and $cb\bar{u}\bar{d}$ systems together with relevant thresholds. The blue lines stand for the tetraquarks including antisymmetric light subsystem $[\bar{u}\bar{d}]$, and the red lines correspond to the ones with symmetric light subsystem $\{\bar{u}\bar{d}\}$.

TABLE VI.   The color proportions and the root mean square radii of the three lowest $cc\bar{u}\bar{d}$, $bb\bar{u}\bar{d}$, and $cb\bar{u}\bar{d}$ states. The expectations $\langle r_{14}^2\rangle^{1/2}$, $\langle r_{23}^2\rangle^{1/2}$, and $\langle r''^2\rangle^{1/2}$ equal to the values of $\langle r_{24}^2\rangle^{1/2}$, $\langle r_{13}^2\rangle^{1/2}$, and $\langle r'^2\rangle^{1/2}$, respectively, which are omitted for simplicity. The units of masses and root mean square radii are in MeV and fm, respectively.

System	Mass	$|\bar{3}3\rangle$	$|6\bar{6}\rangle$	$|11\rangle$	$|88\rangle$	$\langle r_{12}^2\rangle^{1/2}$	$\langle r_{34}^2\rangle^{1/2}$	$\langle r^2\rangle^{1/2}$	$\langle r_{13}^2\rangle^{1/2}$	$\langle r_{24}^2\rangle^{1/2}$	$\langle r'^2\rangle^{1/2}$
$\{cc\}[\bar{u}\bar{d}]$	4041	95.8%	4.2%	34.7%	65.3%	0.449	0.597	0.386	0.537	0.537	0.402
$\{bb\}[\bar{u}\bar{d}]$	10550	99.8%	0.2%	33.4%	66.6%	0.285	0.484	0.370	0.465	0.465	0.274
$(cb)[\bar{u}\bar{d}]$	7297	94.0%	6.0%	35.3%	64.7%	0.357	0.489	0.373	0.521	0.455	0.324

consist of $|(cb)_0^{\bar{3}}[\bar{u}\bar{d}]_0^3\rangle_0$ and $|(cb)_1^{\bar{3}}[\bar{u}\bar{d}]_0^3\rangle_1$ configurations, respectively. The predicted masses of $cb\bar{u}\bar{d}$ tetraquarks are much higher than the $D\bar{B}$ and $D\bar{B}^*$ thresholds, and they can decay via quark rearrangement. Our calculation suggests that no stable $cb\bar{u}\bar{d}$ state does exist.

Together with the mass spectra, the wave functions are also obtained by solving the generalized eigenvalue problem of Hamiltonian. With these wave functions, we can calculate the proportions of hidden color components and the root mean square radii. Besides the $|\bar{3}3\rangle$ and $|6\bar{6}\rangle$ classifications, one can also define other sets of color representations,

$$|11\rangle = |(Q_1\bar{q}_3)^1(Q_2'\bar{q}_4')^1\rangle, \tag{35}$$

$$|88\rangle = |(Q_1\bar{q}_3)^8(Q_2'\bar{q}_4')^8\rangle, \tag{36}$$

and

$$|1'1'\rangle = |(Q_1\bar{q}_4')^1(Q_2'\bar{q}_3)^1\rangle, \tag{37}$$

$$|8'8'\rangle = |(Q_1\bar{q}_4')^8(Q_2'\bar{q}_3)^8\rangle. \tag{38}$$

With the above definitions, the explicit color wave functions can be obtained via the Clebsch-Gordan coefficients of SU(3) group [96,97], and the three sets of color representations can be related as follows [28]:
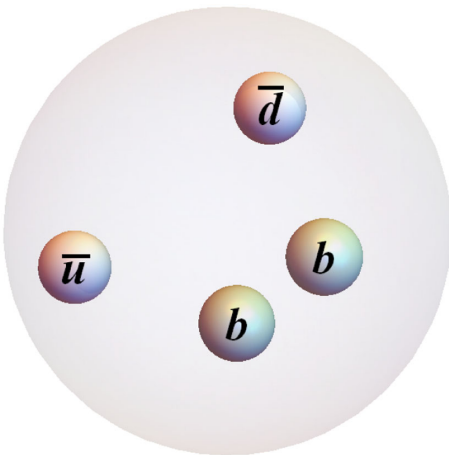
FIG. 4.   The stable $IJ^P = 01^+$ $bb\bar{u}\bar{d}$ state.

$$|11\rangle = \sqrt{\frac{1}{3}}|\bar{3}3\rangle + \sqrt{\frac{2}{3}}|6\bar{6}\rangle, \tag{39}$$

$$|88\rangle = -\sqrt{\frac{2}{3}}|\bar{3}3\rangle + \sqrt{\frac{1}{3}}|6\bar{6}\rangle, \tag{40}$$

and

$$|1'1'\rangle = -\sqrt{\frac{1}{3}}|\bar{3}3\rangle + \sqrt{\frac{2}{3}}|6\bar{6}\rangle, \tag{41}$$

$$|8'8'\rangle = \sqrt{\frac{2}{3}}|\bar{3}3\rangle + \sqrt{\frac{1}{3}}|6\bar{6}\rangle. \tag{42}$$

Here, we adopt the $|11\rangle$ and $|88\rangle$ representations to stand for the neutral color and hidden color components, respectively.

The color proportions and root mean square radii of the three lowest $cc\bar{u}\bar{d}$, $bb\bar{u}\bar{d}$, and $cb\bar{u}\bar{d}$ states are presented in Table VI. The large hidden color component and small root mean square radius indicate that the $IJ^P = 01^+$ $bb\bar{u}\bar{d}$ state is a compact tetraquark rather than a loosely bound molecule. Also, the 0.285–0.484 fm radii differentiate it from a pointlike diquark-antidiquark structure. The sketch of this stable $T_{QQ'}$ state is presented in Fig. 4. It can be seen that the two heavy quarks stay close to each other like a static color source, while the light antiquark pair circles around this source and is shared by two heavy quarks.

C. Strange systems

In present work, we treat the antisymmetric $[\bar{u}\bar{s}]$ and symmetric $\{\bar{u}\bar{s}\}$ as different flavor parts and do not consider the admixture between them. This situation is similar as the conventional $\Xi_{c(b)}$ and $\Xi'_{c(b)}$ baryons, which are usually regarded as two independent families. The mass spectra for the $cc\bar{u}\bar{s}$, $bb\bar{u}\bar{s}$, and $cb\bar{u}\bar{s}$ systems are shown in Table VII and Fig. 5. All of the tetraquarks locate above the corresponding thresholds, and the three lowest ones for these systems are 4232, 10734, and 7483 MeV, respectively. Analogously, the 0^+ and 2^+ states can decay into a pair of pseudoscalar mesons, and the 1^+ states can fall apart into a vector meson plus a pseudoscalar one.

It should be mentioned that in the literature some results supported a stable $\{bb\}[\bar{u}\bar{s}]$ state with $IJ^P = \frac{1}{2}1^+$

TABLE VII. Predicted mass spectra for the $cc\bar{u}\,\bar{s}$, $bb\bar{u}\,\bar{s}$, and $cb\bar{u}\,\bar{s}$ systems.

IJ^P	Configuration	$\langle H \rangle$ (MeV)	Mass (MeV)	Eigenvector
$\frac{1}{2}1^+$	$\|\{cc\}_1^{\bar{3}}[\bar{u}\,\bar{s}]_0^3\rangle_1$ $\|\{cc\}_0^6[\bar{u}\,\bar{s}]_1^{\bar{6}}\rangle_1$	$\begin{pmatrix} 4246 & -50 \\ -50 & 4414 \end{pmatrix}$	$\begin{bmatrix} 4232 \\ 4427 \end{bmatrix}$	$\begin{bmatrix} (-0.965, -0.263) \\ (0.263, -0.965) \end{bmatrix}$
$\frac{1}{2}0^+$	$\|\{cc\}_1^{\bar{3}}\{\bar{u}\,\bar{s}\}_1^3\rangle_0$ $\|\{cc\}_0^6\{\bar{u}\,\bar{s}\}_0^{\bar{6}}\rangle_0$	$\begin{pmatrix} 4370 & -82 \\ -82 & 4465 \end{pmatrix}$	$\begin{bmatrix} 4323 \\ 4512 \end{bmatrix}$	$\begin{bmatrix} (-0.865, -0.501) \\ (0.501, -0.865) \end{bmatrix}$
$\frac{1}{2}1^+$	$\|\{cc\}_1^{\bar{3}}\{\bar{u}\,\bar{s}\}_1^3\rangle_1$	4394	4394	1
$\frac{1}{2}2^+$	$\|\{cc\}_1^{\bar{3}}\{\bar{u}\,\bar{s}\}_1^3\rangle_2$	4440	4440	1
$\frac{1}{2}1^+$	$\|\{bb\}_1^{\bar{3}}[\bar{u}\,\bar{s}]_0^3\rangle_1$ $\|\{bb\}_0^6[\bar{u}\,\bar{s}]_1^{\bar{6}}\rangle_1$	$\begin{pmatrix} 10736 & -19 \\ -19 & 11044 \end{pmatrix}$	$\begin{bmatrix} 10734 \\ 11046 \end{bmatrix}$	$\begin{bmatrix} (-0.998, -0.060) \\ (0.060, -0.998) \end{bmatrix}$
$\frac{1}{2}0^+$	$\|\{bb\}_1^{\bar{3}}\{\bar{u}\,\bar{s}\}_1^3\rangle_0$ $\|\{bb\}_0^6\{\bar{u}\,\bar{s}\}_0^{\bar{6}}\rangle_0$	$\begin{pmatrix} 10888 & 29 \\ 29 & 11094 \end{pmatrix}$	$\begin{bmatrix} 10883 \\ 11098 \end{bmatrix}$	$\begin{bmatrix} (-0.990, 0.138) \\ (-0.138, -0.990) \end{bmatrix}$
$\frac{1}{2}1^+$	$\|\{bb\}_1^{\bar{3}}\{\bar{u}\,\bar{s}\}_1^3\rangle_1$	10897	10897	1
$\frac{1}{2}2^+$	$\|\{bb\}_1^{\bar{3}}\{\bar{u}\,\bar{s}\}_1^3\rangle_2$	10915	10915	1
$\frac{1}{2}0^+$	$\|(cb)_0^{\bar{3}}[\bar{u}\,\bar{s}]_0^3\rangle_0$ $\|(cb)_1^6[\bar{u}\,\bar{s}]_1^{\bar{6}}\rangle_0$	$\begin{pmatrix} 7502 & 61 \\ 61 & 7673 \end{pmatrix}$	$\begin{bmatrix} 7483 \\ 7693 \end{bmatrix}$	$\begin{bmatrix} (-0.952, 0.306) \\ (-0.306, -0.952) \end{bmatrix}$
$\frac{1}{2}1^+$	$\|(cb)_1^{\bar{3}}[\bar{u}\,\bar{s}]_0^3\rangle_1$ $\|(cb)_0^6[\bar{u}\,\bar{s}]_1^{\bar{6}}\rangle_1$ $\|(cb)_1^6[\bar{u}\,\bar{s}]_1^{\bar{6}}\rangle_1$	$\begin{pmatrix} 7519 & 32 & 15 \\ 32 & 7761 & -16 \\ 15 & -16 & 7717 \end{pmatrix}$	$\begin{bmatrix} 7514 \\ 7714 \\ 7769 \end{bmatrix}$	$\begin{bmatrix} (-0.987, 0.134, 0.086) \\ (0.117, 0.249, 0.961) \\ (0.107, 0.959, -0.262) \end{bmatrix}$
$\frac{1}{2}2^+$	$\|(cb)_1^6[\bar{u}\,\bar{s}]_1^{\bar{6}}\rangle_2$	7796	7796	1
$\frac{1}{2}0^+$	$\|(cb)_1^{\bar{3}}\{\bar{u}\,\bar{s}\}_1^3\rangle_0$ $\|(cb)_0^6\{\bar{u}\,\bar{s}\}_0^{\bar{6}}\rangle_0$	$\begin{pmatrix} 7659 & 52 \\ 52 & 7811 \end{pmatrix}$	$\begin{bmatrix} 7643 \\ 7827 \end{bmatrix}$	$\begin{bmatrix} (-0.955, 0.297) \\ (-0.297, -0.955) \end{bmatrix}$
$\frac{1}{2}1^+$	$\|(cb)_0^{\bar{3}}\{\bar{u}\,\bar{s}\}_1^3\rangle_1$ $\|(cb)_1^{\bar{3}}\{\bar{u}\,\bar{s}\}_1^3\rangle_1$ $\|(cb)_1^6\{\bar{u}\,\bar{s}\}_0^{\bar{6}}\rangle_1$	$\begin{pmatrix} 7674 & -9 & -30 \\ -9 & 7675 & -14 \\ -30 & -14 & 7808 \end{pmatrix}$	$\begin{bmatrix} 7659 \\ 7682 \\ 7816 \end{bmatrix}$	$\begin{bmatrix} (0.769, 0.604, 0.211) \\ (0.608, -0.792, 0.053) \\ (-0.199, -0.087, 0.976) \end{bmatrix}$
$\frac{1}{2}2^+$	$\|(cb)_1^{\bar{3}}\{\bar{u}\,\bar{s}\}_1^3\rangle_2$	7705	7705	1

[25,35,46,49,66,67], and others predicted a state near the open bottom thresholds [30,63]. Our results show that the lowest $\{bb\}[\bar{u}\,\bar{s}]$ state is about 40 MeV above the $\bar{B}_s\bar{B}^*$ and $\bar{B}_s^*\bar{B}$ thresholds. Considering the uncertainties of relativized quark model, we conclude that a resonancelike $\{bb\}[\bar{u}\,\bar{s}]$ structure may exist. The results of color proportions and root mean square radii of the three lowest $cc\bar{u}\,\bar{s}$, $bb\bar{u}\,\bar{s}$, and $cb\bar{u}\,\bar{s}$ states are also listed in Table VIII for reference. Our prediction for the lowest $bb\bar{u}\,\bar{s}$ state is higher than the results of lattice QCD and nonrelativistic calculations, which may arise from the relativistic effects in the relativized quark model. Actually, current experimental data for
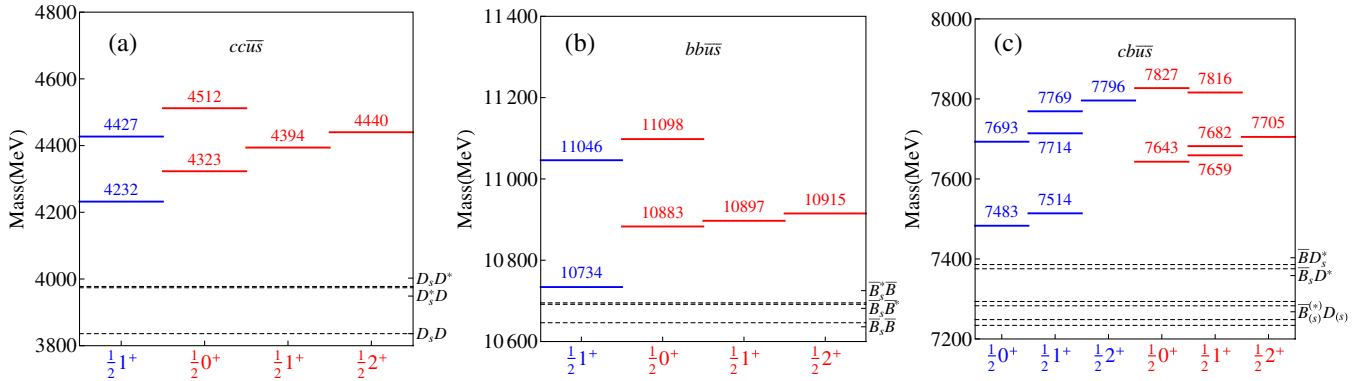
FIG. 5.   The predicted masses of $cc\bar{u}\,\bar{s}$, $bb\bar{u}\,\bar{s}$, and $cb\bar{u}\,\bar{s}$ systems together with relevant thresholds. The blue lines stand for the tetraquarks including antisymmetric light subsystem $[\bar{u}\,\bar{s}]$, and the red lines correspond to the ones with symmetric light subsystem $\{\bar{u}\,\bar{s}\}$.

TABLE VIII. The color proportions and root mean square radii of the three lowest $cc\bar{u}\,\bar{s}$, $bb\bar{u}\,\bar{s}$, and $cb\bar{u}\,\bar{s}$ states. The units of masses and root mean square radii are in MeV and fm, respectively.

System	Mass	$\lvert \bar{3}3\rangle$	$\lvert 6\bar{6}\rangle$	$\lvert 11\rangle$	$\lvert 88\rangle$	$\langle r_{12}^2\rangle^{1/2}$	$\langle r_{34}^2\rangle^{1/2}$	$\langle r^2\rangle^{1/2}$	$\langle r_{13}^2\rangle^{1/2}$	$\langle r_{24}^2\rangle^{1/2}$	$\langle r'^2\rangle^{1/2}$
$\{cc\}[\bar{u}\,\bar{s}]$	4232	93.1%	6.9%	35.6%	64.4%	0.423	0.491	0.384	0.544	0.470	0.363
$\{bb\}[\bar{u}\,\bar{s}]$	10734	99.6%	0.4%	33.5%	66.5%	0.284	0.484	0.364	0.503	0.425	0.269
$(cb)[\bar{u}\,\bar{s}]$	7483	90.6%	9.4%	36.5%	63.5%	0.358	0.493	0.365	0.557	0.412	0.324

TABLE IX. Predicted mass spectra for the $cc\bar{s}\,\bar{s}$, $bb\bar{s}\,\bar{s}$, and $cb\bar{s}\,\bar{s}$ systems.

IJ^P	Configuration	$\langle H\rangle$ (MeV)	Mass (MeV)	Eigenvector
00^+	$\lvert\{cc\}_1^{\bar{3}}\{\bar{s}\,\bar{s}\}_1^{3}\rangle_0$ $\lvert\{cc\}_0^{6}\{\bar{s}\,\bar{s}\}_0^{\bar{6}}\rangle_0$	$\begin{pmatrix} 4469 & 79 \\ 79 & 4535 \end{pmatrix}$	$\begin{bmatrix} 4417 \\ 4587 \end{bmatrix}$	$\begin{bmatrix} (-0.832, 0.555) \\ (-0.555, -0.832) \end{bmatrix}$
01^+	$\lvert\{cc\}_1^{\bar{3}}\{\bar{s}\,\bar{s}\}_1^{3}\rangle_1$	4493	4493	1
02^+	$\lvert\{cc\}_1^{\bar{3}}\{\bar{s}\,\bar{s}\}_1^{3}\rangle_2$	4536	4536	1
00^+	$\lvert\{bb\}_1^{\bar{3}}\{\bar{s}\,\bar{s}\}_1^{3}\rangle_0$ $\lvert\{bb\}_0^{6}\{\bar{s}\,\bar{s}\}_0^{\bar{6}}\rangle_0$	$\begin{pmatrix} 10977 & -29 \\ -29 & 11151 \end{pmatrix}$	$\begin{bmatrix} 10972 \\ 11155 \end{bmatrix}$	$\begin{bmatrix} (-0.987, -0.159) \\ (0.159, -0.987) \end{bmatrix}$
01^+	$\lvert\{bb\}_1^{\bar{3}}\{\bar{s}\,\bar{s}\}_1^{3}\rangle_1$	10986	10986	1
02^+	$\lvert\{bb\}_1^{\bar{3}}\{\bar{s}\,\bar{s}\}_1^{3}\rangle_2$	11004	11004	1
00^+	$\lvert(cb)_1^{\bar{3}}\{\bar{s}\,\bar{s}\}_1^{3}\rangle_0$ $\lvert(cb)_0^{6}\{\bar{s}\,\bar{s}\}_0^{\bar{6}}\rangle_0$	$\begin{pmatrix} 7753 & -50 \\ -50 & 7876 \end{pmatrix}$	$\begin{bmatrix} 7735 \\ 7894 \end{bmatrix}$	$\begin{bmatrix} (-0.941, -0.337) \\ (0.337, -0.941) \end{bmatrix}$
01^+	$\lvert(cb)_0^{\bar{3}}\{\bar{s}\,\bar{s}\}_1^{3}\rangle_1$ $\lvert(cb)_1^{\bar{3}}\{\bar{s}\,\bar{s}\}_1^{3}\rangle_1$ $\lvert(cb)_1^{6}\{\bar{s}\,\bar{s}\}_0^{\bar{6}}\rangle_1$	$\begin{pmatrix} 7767 & -8 & 29 \\ -8 & 7769 & 13 \\ 29 & 13 & 7873 \end{pmatrix}$	$\begin{bmatrix} 7752 \\ 7775 \\ 7881 \end{bmatrix}$	$\begin{bmatrix} (0.784, 0.570, -0.248) \\ (-0.576, 0.816, 0.056) \\ (-0.234, -0.099, -0.967) \end{bmatrix}$
02^+	$\lvert(cb)_1^{\bar{3}}\{\bar{s}\,\bar{s}\}_1^{3}\rangle_2$	7798	7798	1

mesons cannot distinguish the nonrelativistic Cornell potential and relativized potential, since both of them can describe the low-lying meson spectra. Thus, the tetraquark spectra may provide a good platform to test their reasonability. More experimental searches are expected to resolve this problem in the future.

For the $cc\bar{s}\,\bar{s}$, $bb\bar{s}\,\bar{s}$, and $cb\bar{s}\,\bar{s}$ systems, the strange quark pair must be symmetric in flavor part and therefore, less states are predicted. From Table IX and Fig. 6, It can been seen that all of them lie much higher than the corresponding

thresholds and can easily fall apart into the charmed strange or bottom strange final states. Our results are consistent with other theoretical works [30,40], and we believe that no stable structure exists in $cc\bar{s}\,\bar{s}$, $bb\bar{s}\,\bar{s}$, and $cb\bar{s}\,\bar{s}$ systems.

D. Mass ratios

With the mass spectra of the doubly heavy tetraquarks $T_{QQ'}$, one can discuss the mass differences between tetraquark states and the corresponding thresholds. For instance,
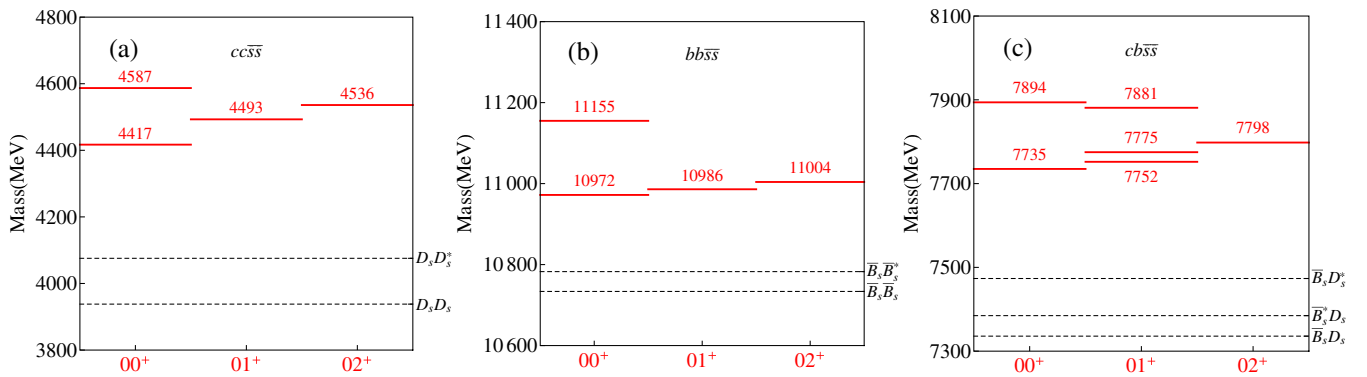
FIG. 6. The predicted masses of the $cc\bar{s}\,\bar{s}$, $bb\bar{s}\,\bar{s}$, and $cb\bar{s}\,\bar{s}$ systems together with relevant thresholds.
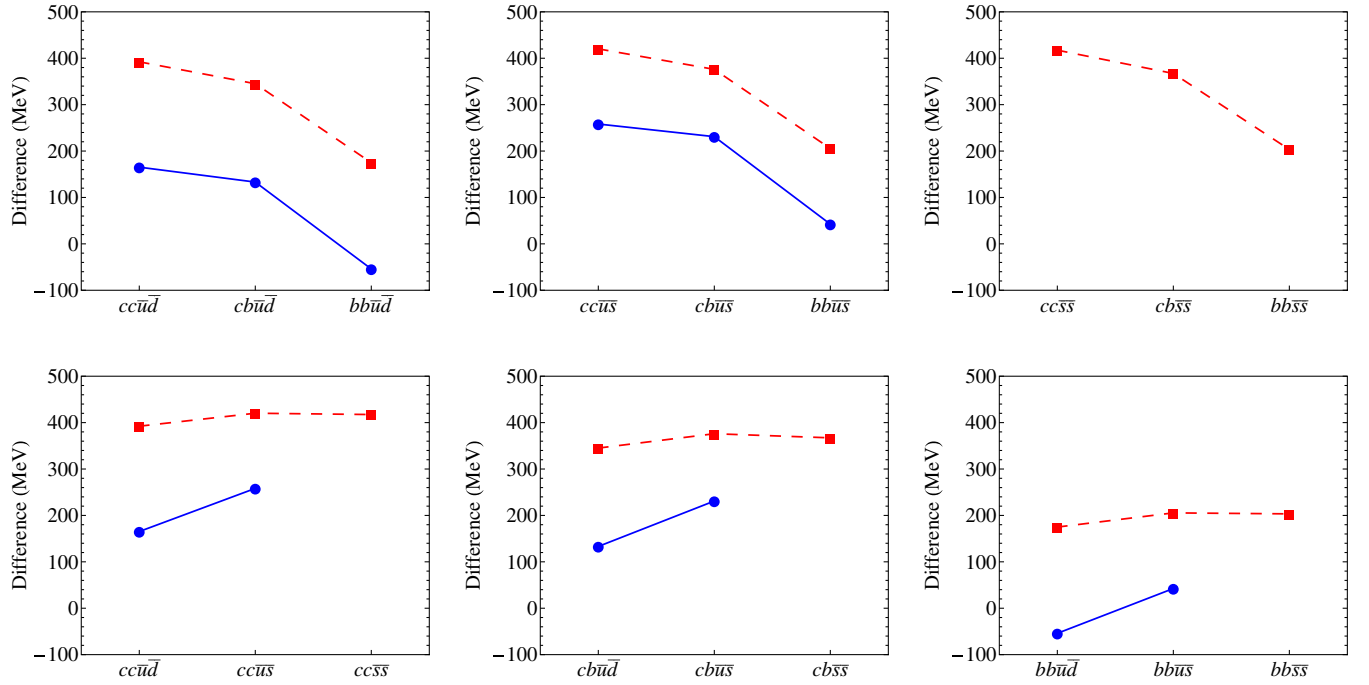
FIG. 7.   Mass differences between lower $J^P = 1^+$ tetraquarks and thresholds versus the different systems. The blue points stand for the tetraquarks including antisymmetric light subsystems, and the red squares correspond to the ones with symmetric light subsystems.

the mass differences between lower $J^P = 1^+$ tetraquarks and thresholds versus the different systems are plotted in Fig. 7. With the fixed light antiquark subsystem, the mass differences decrease when the heavy quarks vary from cc to bb. Similarly, for a certain heavy quark subsystem, the mass differences show upward trends when the light antiquarks change from the $\bar{u}\,\bar{d}$ to $\bar{s}\,\bar{s}$. The $IJ^P = 01^+$ $\{bb\}[\bar{u}\,\bar{d}]$ state has the largest mass ratio between heavy quarks and light antiquarks, which forms a binding compact tetraquark. With the mass ratios between two subsystems decreasing, we can not obtain stable doubly heavy tetraquarks.

In Refs. [41,78], the authors also discussed the dependence of mass ratios between the heavy and light subsystems within nonrelativistic quark model, and showed the same behaviors with our relativized calculations. If one keeps reducing the mass ratios, the doubly heavy tetraquarks will become fully heavy tetraquarks. We can speculate that there is no stable state for the fully heavy tetraquarks since the mass ratios between the two subsystems are sufficiently small. This conjecture is supported by the experimental observations [98,99] and nonrelativistic quark model works with proper potentials [100–105]. Certainly, the classifications of fully heavy tetraquarks are different with doubly heavy tetraquarks; precise calculations within the relativized quark model are needed before coming to any conclusion.

IV. SUMMARY

In this work, we systematically investigate the mass spectra of doubly heavy tetraquarks $T_{QQ'}$ in a relativized quark model. The four-body systems including the

Coulomb potential, confining potential, spin-spin interactions, and relativistic corrections are solved within the variational method. With the present extension, the tetraquark, as well as the conventional hadrons can be described in a uniform frame. Our results suggest that the $IJ^P = 01^+$ $bb\bar{u}\,\bar{d}$ state is 54 MeV below the relevant $\bar{B}\bar{B}^*$ thresholds, which indicates that both strong and electromagnetic decays are forbidden, and thus this state can be a stable one. The large hidden color component and small root mean square radius demonstrate that it is a compact tetraquark rather than a loosely bound molecule or pointlike diquark-antidiquark structure. Compared with the results of nonrelativistic quark models, our calculations present a lower binding energy of this promising isoscalar T_{bb} state, but the decay behaviors agree with each other. We believe our calculations and predictions of the doubly heavy tetraquarks may provide valuable information for future experimental searches.

[1] M. Tanabashi *et al.* (Particle Data Group), Review of particle physics, Phys. Rev. D **98**, 030001 (2018).

[2] H. X. Chen, W. Chen, X. Liu, and S. L. Zhu, The hidden-charm pentaquark and tetraquark states, Phys. Rep. **639**, 1 (2016).

[3] A. Hosaka, T. Iijima, K. Miyabayashi, Y. Sakai, and S. Yasui, Exotic hadrons with heavy flavors: X, Y, Z, and related states, Prog. Theor. Exp. Phys. **2016**, 062C01 (2016).

[4] J. M. Richard, Exotic hadrons: Review and perspectives, Few Body Syst. **57**, 1185 (2016).

[5] R. F. Lebed, R. E. Mitchell, and E. S. Swanson, Heavy-quark QCD exotica, Prog. Part. Nucl. Phys. **93**, 143 (2017).

[6] A. Ali, J. S. Lange, and S. Stone, Exotics: Heavy penta-quarks and tetraquarks, Prog. Part. Nucl. Phys. **97**, 123 (2017).

[7] A. Esposito, A. Pilloni, and A. Polosa, Multiquark reso-nances, Phys. Rep. **668**, 1 (2017).

[8] F. K. Guo, C. Hanhart, U. G. Meißner, Q. Wang, Q. Zhao, and B. S. Zou, Hadronic molecules, Rev. Mod. Phys. **90**, 015004 (2018).

[9] S. L. Olsen, T. Skwarnicki, and D. Zieminska, Nonstand-ard heavy mesons and baryons: Experimental evidence, Rev. Mod. Phys. **90**, 015003 (2018).

[10] M. Karliner, J. L. Rosner, and T. Skwarnicki, Multiquark states, Annu. Rev. Nucl. Part. Sci. **68**, 17 (2018).

[11] Y. R. Liu, H. X. Chen, W. Chen, X. Liu, and S. L. Zhu, Pentaquark and tetraquark states, Prog. Part. Nucl. Phys. **107**, 237 (2019).

[12] N. Brambilla, S. Eidelman, C. Hanhart, A. Nefediev, C. P. Shen, C. E. Thomas, A. Vairo, and C. Z. Yuan, The *XYZ* states: Experimental and theoretical status and perspec-tives, arXiv:1907.07583.

[13] S. Choi *et al.* (Belle Collaboration), Observation of a Resonance-Like Structure in the $\pi^{\pm}\psi'$ Mass Distribution in Exclusive $B \to K\pi^{\pm}\psi'$ Decays, Phys. Rev. Lett. **100**, 142001 (2008).

[14] R. Aaij *et al.* (LHCb Collaboration), Observation of the Resonant Character of the $Z(4430)^-$ State, Phys. Rev. Lett. **112**, 222002 (2014).

[15] A. Bondar *et al.* (Belle Collaboration), Observation of Two Charged Bottomonium-Like Resonances in $\Upsilon(5S)$ De-cays, Phys. Rev. Lett. **108**, 122001 (2012).

[16] M. Ablikim *et al.* (BESIII Collaboration), Observation of a Charged Charmoniumlike Structure in $e^+e^- \to \pi^+\pi^- J/\psi$ at $\sqrt{s} = 4.26$ GeV, Phys. Rev. Lett. **110**, 252001 (2013).

[17] Z. Liu *et al.* (Belle Collaboration), Study of $e^+e^- \to \pi^+\pi^- J/\psi$ and Observation of a Charged Charmoniumlike State at Belle, Phys. Rev. Lett. **110**, 252002 (2013).

[18] R. Aaij *et al.* (LHCb Collaboration), Observation of $J/\psi p$ Resonances Consistent with Pentaquark States in $\Lambda_b^0 \to J/\psi K^- p$ Decays, Phys. Rev. Lett. **115**, 072001 (2015).

[19] R. Aaij *et al.* (LHCb Collaboration), Observation of a Narrow Pentaquark State, $P_c(4312)^+$, and of Two-Peak Structure of the $P_c(4450)^+$, Phys. Rev. Lett. **122**, 222001 (2019).

[20] T. Nakano *et al.* (LEPS Collaboration), Evidence for a Narrow $S = +1$ Baryon Resonance in Photoproduction from the Neutron, Phys. Rev. Lett. **91**, 012002 (2003).

[21] V. Abazov *et al.* (D0 Collaboration), Evidence for a $B_s^0\pi^{\pm}$ State, Phys. Rev. Lett. **117**, 022003 (2016).

[22] R. Aaij *et al.* (LHCb Collaboration), Search for Structure in the $B_s^0\pi^{\pm}$ Invariant Mass Spectrum, Phys. Rev. Lett. **117**, 152003 (2016).

[23] R. Aaij *et al.* (LHCb Collaboration), Observation of the Doubly Charmed Baryon Ξ_{cc}^{++}, Phys. Rev. Lett. **119**, 112001 (2017).

[24] M. Karliner and J. L. Rosner, Discovery of Doubly-Charmed Ξ_{cc} Baryon Implies a Stable $(bb\bar{u}\bar{d})$ Tetraquark, Phys. Rev. Lett. **119**, 202001 (2017).

[25] E. J. Eichten and C. Quigg, Heavy-Quark Symmetry Implies Stable Heavy Tetraquark Mesons $Q_iQ_j\bar{q}_k\bar{q}_l$, Phys. Rev. Lett. **119**, 202002 (2017).

[26] J. L. Ballot and J. M. Richard, Four quark states in additive potentials, Phys. Lett. **123B**, 449 (1983).

[27] H. J. Lipkin, A model-independent approach to multiquark bound states, Phys. Lett. B **172**, 242 (1986).

[28] J. Vijande and A. Valcarce, Tetraquark spectroscopy: A symmetry analysis, Symmetry **1**, 155 (2009).

[29] S. Q. Luo, K. Chen, X. Liu, Y. R. Liu, and S. L. Zhu, Exotic tetraquark states with the $qq\bar{Q}\bar{Q}$ configuration, Eur. Phys. J. C **77**, 709 (2017).

[30] D. Ebert, R. N. Faustov, V. O. Galkin, and W. Lucha, Masses of tetraquarks with two heavy quarks in the relativistic quark model, Phys. Rev. D **76**, 114015 (2007).

[31] C. Semay and B. Silvestre-Brac, Diquonia and potential models, Z. Phys. C **61**, 271 (1994).

[32] S. Zouzou, B. Silvestre-Brac, C. Gignoux, and J. M. Richard, Four quark bound states, Z. Phys. C **30**, 457 (1986).

[33] L. Heller and J. A. Tjon, On the existence of stable dimesons, Phys. Rev. D **35**, 969 (1987).

[34] J. Carlson, L. Heller, and J. A. Tjon, Stability of dimesons, Phys. Rev. D **37**, 744 (1988).

[35] B. Silvestre-Brac and C. Semay, Systematics of $L = 0$ $q^2\bar{q}^2$ systems, Z. Phys. C **57**, 273 (1993).

[36] B. Silvestre-Brac and C. Semay, Spectrum and decay properties of diquonia, Z. Phys. C **59**, 457 (1993).

[37] S. Pepin, F. Stancu, M. Genovese, and J. M. Richard, Tetraquarks with color blind forces in chiral quark models, Phys. Lett. B **393**, 119 (1997).

[38] D. M. Brink and F. Stancu, Tetraquarks with heavy flavors, Phys. Rev. D **57**, 6778 (1998).

[39] J. Vijande, F. Fernandez, A. Valcarce, and B. Silvestre-Brac, Tetraquarks in a chiral constituent quark model, Eur. Phys. J. A **19**, 383 (2004).

[40] M. Zhang, H. X. Zhang, and Z. Y. Zhang, $QQ\bar{q}\bar{q}$ four-quark bound states in chiral SU(3) quark model, Commun. Theor. Phys. **50**, 437 (2008).

[41] J. Vijande, A. Valcarce, and N. Barnea, Exotic meson-meson molecules and compact four-quark states, Phys. Rev. D **79**, 074010 (2009).

[42] Y. C. Yang, C. R. Deng, J. L. Ping, and T. Goldman, S-wave $QQ\bar{q}\bar{q}$ state in the constituent quark model, Phys. Rev. D **80**, 114023 (2009).

[43] F. S. Navarra, M. Nielsen, and S. H. Lee, QCD sum rules study of $QQ - \bar{u}\bar{d}$ mesons, Phys. Lett. B **649**, 166 (2007).

[44] J. M. Dias, S. Narison, F. S. Navarra, M. Nielsen, and J.-M. Richard, Relation between $T_{cc,bb}$ and $X_{c,b}$ from QCD, Phys. Lett. B **703,** 274 (2011).

[45] W. Chen, T. G. Steele, and S. L. Zhu, Exotic open-flavor $bc\bar{q}\,\bar{q}$, $bc\bar{s}\,\bar{s}$ and $qc\bar{q}\,\bar{b}$, $sc\bar{s}\,\bar{b}$ tetraquark states, Phys. Rev. D **89,** 054037 (2014).

[46] M. L. Du, W. Chen, X. L. Chen, and S. L. Zhu, Exotic $QQ\bar{q}\,\bar{q}$, $QQ\bar{q}\,\bar{s}$ and $QQ\bar{s}\,\bar{s}$ states, Phys. Rev. D **87,** 014003 (2013).

[47] Y. Ikeda, B. Charron, S. Aoki, T. Doi, T. Hatsuda, T. Inoue, N. Ishii, K. Murano, H. Nemura, and K. Sasaki, Charmed tetraquarks T_{cc} and T_{cs} from dynamical lattice QCD simulations, Phys. Lett. B **729,** 85 (2014).

[48] P. Bicudo, K. Cichy, A. Peters, and M. Wagner, BB interactions with static bottom quarks from Lattice QCD, Phys. Rev. D **93,** 034501 (2016).

[49] A. Francis, R. J. Hudspith, R. Lewis, and K. Maltman, Lattice Prediction for Deeply Bound Doubly Heavy Tetraquarks, Phys. Rev. Lett. **118,** 142001 (2017).

[50] P. Bicudo, M. Cardoso, A. Peters, M. Pflaumer, and M. Wagner, $ud\bar{b}\,\bar{b}$ tetraquark resonances with lattice QCD potentials and the Born-Oppenheimer approximation, Phys. Rev. D **96,** 054510 (2017).

[51] B. A. Gelman and S. Nussinov, Does a narrow tetraquark $cc\bar{u}\,\bar{d}$ state exist?, Phys. Lett. B **551,** 296 (2003).

[52] D. Janc and M. Rosina, The $T_{cc} = DD^*$ molecular state, Few Body Syst. **35,** 175 (2004).

[53] A. Del Fabbro, D. Janc, M. Rosina, and D. Treleani, Production and detection of doubly charmed tetraquarks, Phys. Rev. D **71,** 014008 (2005).

[54] Y. Q. Chen and S. Z. Wu, Production of four-quark states with double heavy quarks at LHC, Phys. Lett. B **705,** 93 (2011).

[55] T. Hyodo, Y. R. Liu, M. Oka, K. Sudoh, and S. Yasui, Production of doubly charmed tetraquarks with exotic color configurations in electron-positron collisions, Phys. Lett. B **721,** 56 (2013).

[56] T. Mehen, Implications of heavy quark-diquark symmetry for excited doubly heavy baryons and tetraquarks, Phys. Rev. D **96,** 094028 (2017).

[57] Z. G. Wang and Z. H. Yan, Analysis of the scalar, axia-lvector, vector, tensor doubly charmed tetraquark states with QCD sum rules, Eur. Phys. J. C **78,** 19 (2018).

[58] X. J. Yan, B. Zhong, and R. L. Zhu, Doubly charmed tetraquarks in a diquark-antidiquark model, Int. J. Mod. Phys. A **33,** 1850096 (2018).

[59] A. Ali, A. Y. Parkhomenko, Q. Qin, and W. Wang, Prospects of discovering stable double-heavy tetraquarks at a tera-Z factory, Phys. Lett. B **782,** 412 (2018).

[60] Y. Xing and R. Zhu, Weak decays of stable doubly heavy tetraquark states, Phys. Rev. D **98,** 053005 (2018).

[61] S. S. Agaev, K. Azizi, B. Barsbay, and H. Sundu, The doubly charmed pseudoscalar tetraquarks $T^{++}_{cc;\bar{s}\,\bar{s}}$ and $T^{++}_{cc;\bar{d}\,\bar{s}}$, Nucl. Phys. **B939,** 130 (2019).

[62] A. Ali, Q. Qin, and W. Wang, Discovery potential of stable and near-threshold doubly heavy tetraquarks at the LHC, Phys. Lett. B **785,** 605 (2018).

[63] W. Park, S. Noh, and S. H. Lee, Masses of the doubly heavy tetraquarks in a constituent quark model, Nucl. Phys. **A983,** 1 (2019).

[64] S. S. Agaev, K. Azizi, B. Barsbay, and H. Sundu, Weak decays of the axial-vector tetraquark $T^{-}_{bb;\bar{u}\,\bar{d}}$, Phys. Rev. D **99,** 033002 (2019).

[65] A. Francis, R. J. Hudspith, R. Lewis, and K. Maltman, Evidence for charm-bottom tetraquarks and the mass dependence of heavy-light tetraquark states from lattice QCD, Phys. Rev. D **99,** 054505 (2019).

[66] P. Junnarkar, N. Mathur, and M. Padmanath, Study of doubly heavy tetraquarks in Lattice QCD, Phys. Rev. D **99,** 034507 (2019).

[67] C. R. Deng, H. Chen, and J. L. Ping, Systematical investigation on the stability of doubly heavy tetraquark states, Eur. Phys. J. A **56,** 9 (2020).

[68] T. F. Carames, J. Vijande, and A. Valcarce, Exotic $bc\bar{q}\,\bar{q}$ four-quark states, Phys. Rev. D **99,** 014006 (2019).

[69] S. S. Agaev, K. Azizi, and H. Sundu, Strong decays of double-charmed pseudoscalar and scalar $cc\bar{u}\,\bar{d}$ tetraquarks, Phys. Rev. D **99,** 114016 (2019).

[70] H. Sundu, S. S. Agaev, and K. Azizi, Semileptonic decays of the scalar tetraquark $Z^0_{bc;\bar{u}\,\bar{d}}$, Eur. Phys. J. C **79,** 753 (2019).

[71] L. Maiani, A. D. Polosa, and V. Riquer, Hydrogen bond of QCD, Phys. Rev. D **100,** 014002 (2019).

[72] R. L. Zhu, X. J. Liu, H. X. Huang, and C. F. Qiao, Analyzing doubly heavy tetra- and penta-quark states by variational method, Phys. Lett. B **797,** 134869 (2019).

[73] L. Maiani, A. D. Polosa, and V. Riquer, Hydrogen bond of QCD in doubly heavy baryons and tetraquarks, Phys. Rev. D **100,** 074002 (2019).

[74] C. E. Fontoura, G. Krein, A. Valcarce, and J. Vijande, Production of exotic tetraquarks $QQ\bar{q}\,\bar{q}$ in heavy-ion collisions at the LHC, Phys. Rev. D **99,** 094037 (2019).

[75] S. Agaev, K. Azizi, and H. Sundu, Double-heavy axial-vector tetraquark $T^0_{bc;\bar{u}\,\bar{d}}$, Nucl. Phys. **B951,** 114890 (2020).

[76] L. Leskovec, S. Meinel, M. Pflaumer, and M. Wagner, Lattice QCD investigation of a doubly-bottom $\bar{b}\,\bar{b}\,ud$ tetraquark with quantum numbers $I(J^P) = 0(1^+)$, Phys. Rev. D **100,** 014503 (2019).

[77] Y. Liu, M. A. Nowak, and I. Zahed, Heavy tetraquark $QQ\bar{q}\,\bar{q}$ as a hadronic Efimov state, arXiv:1909.02497.

[78] E. Hernandez, J. Vijande, A. Valcarce, and J. M. Richard, Spectroscopy, lifetime and decay modes of the T^{-}_{bb} tetraquark, Phys. Lett. B **800,** 135073 (2020).

[79] G. Yang, J. L. Ping, and J. Segovia, Doubly-heavy tetra-quarks, Phys. Rev. D **101,** 014001 (2020).

[80] L. Tang, B. D. Wan, K. Maltman, and C. F. Qiao, Doubly heavy tetraquarks in QCD sum rules, Phys. Rev. D **101,** 094032 (2020).

[81] S. Agaev, K. Azizi, B. Barsbay, and H. Sundu, Stable scalar tetraquark $T^{-}_{bb;\bar{u}\,\bar{d}}$, arXiv:2001.01446.

[82] Q. N. Wang and W. Chen, Fully open-flavor tetraquark states $bc\bar{q}\,\bar{s}$ and $sc\bar{q}\,\bar{b}$ with $J^P = 0^+, 1^+$, Eur. Phys. J. C **80,** 389 (2020).

[83] Y. Tan, W. Lu, and J. L. Ping, $QQ\bar{q}\,\bar{q}$ in a chiral constituent quark model, arXiv:2004.02106.

[84] S. Godfrey and N. Isgur, Mesons in a relativized quark model with chromodynamics, Phys. Rev. D **32,** 189 (1985).

[85] S. Capstick and N. Isgur, Baryons in a relativized quark model with chromodynamics, Phys. Rev. D **34,** 2809 (1986).

[86] Q. F. Lü and Y. B. Dong, $X(4140)$, $X(4274)$, $X(4500)$, and $X(4700)$ in the relativized quark model, Phys. Rev. D **94,** 074007 (2016).

[87] Q. F. Lü and Y. B. Dong, Masses of open charm and bottom tetraquark states in a relativized quark model, Phys. Rev. D **94,** 094041 (2016).

[88] Q. F. Lü, K. L. Wang, and Y. B. Dong, The $ss\bar{s}\,\bar{s}$ tetraquark states and the newly observed structure $X(2239)$ by BESIII Collaboration, Chin. Phys. C **44,** 024101 (2020).

[89] M. N. Anwar, J. Ferretti, F. K. Guo, E. Santopinto, and B. S. Zou, Spectroscopy and decays of the fully-heavy tetraquarks, Eur. Phys. J. C **78,** 647 (2018).

[90] M. N. Anwar, J. Ferretti, and E. Santopinto, Spectroscopy of the hidden-charm $[qc][\bar{q}\,\bar{c}]$ and $[sc][\bar{s}\,\bar{c}]$ tetraquarks in the relativized diquark model, Phys. Rev. D **98,** 094015 (2018).

[91] M. A. Bedolla, J. Ferretti, C. D. Roberts, and E. Santopinto, Spectrum of fully-heavy tetraquarks from a diquark + antidiquark perspective, arXiv:1911.00960.

[92] J. Ferretti and E. Santopinto, Hidden-charm and bottom tetra- and pentaquarks with strangeness in the hadro-quarkonium and compact tetraquark models, J. High Energy Phys. 04 (2020) 119.

[93] E. Hiyama, Y. Kino, and M. Kamimura, Gaussian expansion method for few-body systems, Prog. Part. Nucl. Phys. **51,** 223 (2003).

[94] R. Aaij *et al.* (LHCb Collaboration), Physics case for an LHCb Upgrade II–Opportunities in flavour physics, and beyond, in the HL-LHC era, arXiv:1808.08865.

[95] A. Cerri *et al.*, Report from working group 4 : Opportunities in flavour Physics at the HL-LHC and HE-LHC, CERN Yellow Rep.Monogr. **7,** 867 (2019).

[96] J. J. de Swart, The octet model and its Clebsch-Gordan coefficients, Rev. Mod. Phys. **35,** 916 (1963); **37,** 326(E) (1965).

[97] T. A. Kaeding, Tables of SU(3) isoscalar factors, At. Data Nucl. Data Tables **61,** 233 (1995).

[98] R. Aaij *et al.* (LHCb Collaboration), Search for beautiful tetraquarks in the $\Upsilon(1S)\mu^+\mu^-$ invariant-mass spectrum, J. High Energy Phys. 10 (2018) 086.

[99] A. M. Sirunyan *et al.* (CMS Collaboration), Measurement of the $\Upsilon(1S)$ pair production cross section and search for resonances decaying to $\Upsilon(1S)\mu^+\mu^-$ in proton-proton collisions at $\sqrt{s} = 13$ TeV, Phys. Lett. B **808,** 135578 (2020).

[100] J. M. Richard, A. Valcarce, and J. Vijande, String dynamics and metastability of all-heavy tetraquarks, Phys. Rev. D **95,** 054019 (2017).

[101] M. S. Liu, Q. F. Lü, X. H. Zhong, and Q. Zhao, All-heavy tetraquarks, Phys. Rev. D **100,** 016006 (2019).

[102] G. J. Wang, L. Meng, and S. L. Zhu, Spectrum of the fully-heavy tetraquark state $QQ\bar{Q}'\bar{Q}'$, Phys. Rev. D **100,** 096013 (2019).

[103] X. Y. Chen, Fully-heavy tetraquarks: $bb\bar{c}\,\bar{c}$ and $bc\bar{b}\,\bar{c}$, Phys. Rev. D **100,** 094009 (2019).

[104] J. M. Richard, A. Valcarce, and J. Vijande, Hall-Post inequalities: Review and application to molecules and tetraquarks, Ann. Phys. (Amsterdam) **412,** 168009 (2020).

[105] C. R. Deng, H. Chen, and J. L. Ping, Towards the understanding of fully-heavy tetraquark states from various models, arXiv:2003.05154.